Simultaneous Photodissociation of H_2 and PMe_2Ph from $OsH_4(PMe_2Ph)_3$: Production of Dimeric and Paramagnetic Osmium Polyhydrides

Joseph W. Bruno, John C. Huffman, Mark A. Green, Jeffrey D. Zubkowski, William E. Hatfield, and Kenneth G. Caulton*

Department of Chemistry and Molecular Structure Center, Indiana University, Bloomington, Indiana 47405, and Department of Chemistry, University of North Carolina, Chapel Hill, North Carolina 27514

Received March 12, 1990

Chemical trapping with PMe_2Ph ("P"), PEt_3, and H_2 (to 60 atm) has been used to prove the concurrent photodissociation of both H_2 and PMe_2Ph from OsH_4P_3 in benzene, THF, and ethanol; the ratio of the former to the latter processes is 1:1.7. The final products observed on photolysis of OsH_4P_3 under vacuum is an equilibrium mixture of $Os_2H_4P_6$ and $Os_2H_4P_5$. The crystal structure of the former shows it to be comprised of two octahedra sharing an edge, the edge being composed of two bridging hydrides; the Os–Os distance is 2.818 (1) Å. The structure of an analogue of the latter has been determined: $Os_2H_4(PMePh_2)_5$ has a face-shared octahedral structure with a distance between chemically inequivalent osmiums of 2.551 (1) Å. By a study of the photolysis of $OsH_4(PEt_3)_3$, which shows PEt_3 dissociation but no H_2 dissociation, it was concluded that a transient dihydride is the crucial intermediate in leading to dimeric products. Dimeric $Os_2H_4P_6$ is itself photosensitive, leading to products of P–CH_3 cleavage ($Os_2H_4(PMe_2Ph)_4(\mu$-$PMePh)_2$), as well as to a product of Os–H *heterolysis*, $[Os_2H_3P_6^+][trans$-$OsH_4P_2^-]$, the latter containing a unique paramagnetic polyhydride anion.

Introduction

The thermal stabilities of transition-metal polyhydrides are often remarkably high, particularly since their decomposition might be anticipated to be driven by the strong bond in the resulting H_2. This apparent stability toward H_2 elimination is exhibited by the series of rhenium polyhydrides ReP_xH_{11-2x} (x = 2–4), in which only ReH_7P_2 has been shown to be susceptible to thermal H_2 loss.[1,2] As synthesized, these compounds adhere strictly to the effective atomic number (EAN) rule. As a corollary, associative substitution processes are uncommon and the dissociative formation of unsaturated fragments is a necessary preliminary to the binding of Lewis bases to polyhydrides. Photochemical activation has proven useful in generating kinetically significant intermediates.[3] For compounds with hydride ligands in cis positions, H_2 elimination is often the primary photochemical event, and the resulting unsaturated fragments have proven very reactive. However, the compound ReH_5P_3 (P = PMe_2Ph) is most unusual in polyhydride chemistry in that phosphine dissociation is the only operative photoprocess.[4,5] This yields the transient ReH_5P_2, which is capable of effecting H/D exchange in both aromatic and aliphatic systems. Ultimately, the 16-electron transient ReH_5P_2 leads to the production of $Re_2(\mu$-$H)_4H_4P_4$ (1) and $Re_2(\mu$-$H)_3H_3P_5$ (2), both of which contain a Re–Re triple bond.

The foregoing discussion indicates the utility of polyhydrides in the production of hydride-rich dimers containing metal–metal bonds. Also evident is the fact that not only H_2 dissociation but also phosphine dissociation must be considered in assessing the photochemistry of polyhydrides. It is against this background that we have turned our attention to a study of the photochemistry of OsH_4P_3, a compound first reported by Shaw and coworkers.[6,7] In particular, we sought to establish the primary photochemical event, as well as the products resulting therefrom. Herein, we report the results of our studies; part of this work has been presented in a preliminary communication.[8]

*To whom correspondence should be addressed at Indiana University.

Results

Characterization of $OsH_4(PMe_2Ph)_3$. The molecular structure of $OsH_4(PMe_2Ph)_3$ has been determined by neutron diffraction.[9] It is suitably described as a pentagonal bipyramid in which the σ-donor hydride ligands are all contained in the pentagonal plane. One phosphine resides in this plane, and the other two occupy axial positions. Since the bulky phosphines constitute a pseudomeridional array, there is a distortion of the two axial phosphines away from the equatorial phosphine and toward the four hydrides. Although $OsH_4(PMe_2Ph)_3$ is fluxional to the point of showing only an Os–H ^1H NMR quartet and a $^{31}P\{^1H\}$ singlet at 25 °C, we have confirmed the persistence of the solid-state structure in toluene-d_8/CF_2Cl_2 solution by observing two equally intense hydride resonances and 2:1 ^{31}P resonances at −120 °C. Clearly, the existence of cis hydrides in $OsH_4(PMe_2Ph)_3$ is ample reason to consider possible photochemical H_2 loss from OsH_4P_3. Irradiation is essential to eliciting the chemistry we describe here; refluxing OsH_4P_3 for 24 h in toluene produces no change, the tetrahydride being quantitatively recovered.

In addition to a high-energy continuum, the UV–visible spectrum of $OsH_4(PMe_2Ph)_3$ in pentane exhibits a strong absorption (ϵ = 5400 L/(mol cm)) at 282 nm. The compound is photostable in Pyrex glassware, which is opaque below ca. 300 nm. The photochemistry reported here was performed with quartz glassware, by use of either high-

(1) Hlatky, G. E.; Crabtree, R. H. *Coord. Chem. Rev.* **1985**, *65*, 1.
(2) Makhaev, V. D.; Borisov, A. P. *Russ. Chem. Rev.* (*Engl. Transl.*) **1988**, *57*, 1162.
(3) Geoffroy, G. L.; Wrighton, M. S. *Organometallic Photochemistry*; Academic Press: New York, 1979.
(4) Roberts, D. A.; Geoffroy, G. L. *J. Organomet. Chem.* **1981**, *214*, 221.
(5) Green, M. A.; Huffman, J. C; Caulton, K. G. *J. Am. Chem. Soc.* **1981**, *103*, 695.
(6) Douglas, P. G.; Shaw, B. L. *J. Chem. Soc. A.* **1970**, 334.
(7) Bell, G.; Chatt, J.; Leigh, G. L. *J. Chem. Soc., Dalton Trans.* **1973**, 997.
(8) Green, M. A.; Huffman, J. C.; Caulton, K. G. *J. Organomet. Chem.* **1983**, *243*, C78.
(9) Hart, D. W.; Bau, R.; Koetzle, T. F. *J. Am. Chem. Soc.* **1977**, *99*, 7557.

0276-7333/90/2309-2556$02.50/0

pressure or medium-pressure mercury vapor lamps or a monochromatic 254-nm source. The reactions showed no obvious dependence on source (other than that due to intensity differences), and the photochemistry is thought to arise from irradiation into the band at 282 nm.

Scavenging Studies. The photochemistry of OsH_4P_3 was conducted in the presence of reagents chosen to elucidate the reaction pathway. In one experiment, OsH_4P_3 was irradiated (benzene solution) in the presence of 3–4 equiv of added PMe_2Ph. The result was exclusive production of *cis*-$OsH_2(PMe_2Ph)_4$ (eq 1). As reported by

$$OsH_4P_3 + P \xrightarrow[C_6H]{h\nu} \textit{cis}\text{-}OsH_2P_4 + H_2 \qquad (1)$$

Chatt and co-workers,[7] this substitution of phosphine for H_2 is also effected by heating to 100 °C for 20 h. However, there is no thermal pathway contributing in the (25 °C) photochemical study; in the absence of irradiation, a solution of OsH_4P_3 and PMe_2Ph showed no change after 24 h at room temperature.

Equation 1 indicates that dihydrogen loss (eq 2) follows absorption of a photon. To further test this hypothesis,

$$OsH_4P_3 \xrightarrow{h\nu} OsH_2P_3 + H_2 \qquad (2)$$

OsH_4P_3 was irradiated under 1 atm of H_2 in THF. If eq 2 is operative, the presence of added dissolved H_2 might quench the photochemistry (i.e., provide an efficient back-reaction), leaving the system photostable. The photochemical reaction was, however, unaltered from its course under an atmosphere of N_2 (vide infra). On the assumption that failure to quench eq 2 is due to insufficient concentration of dissolved H_2, the same irradiation was studied under 600–900 psi of H_2 in a photochemical pressure reactor. Under these conditions, the system is not photostable, but instead there is complete conversion to OsH_6P_2 and free PMe_2Ph, according to the stoichiometry of eq 3. The former was identified by comparison

$$OsH_4P_3 + H_2\ (40\ atm) \xrightarrow[THF]{h\nu} OsH_6P_2 + P \qquad (3)$$

with a sample prepared from $OsCl_4P_2$ and $NaBH_4$.[6] This result is noteworthy for two reasons. First, the literature synthesis of OsH_6P_2 affords the compound in ca. 40% yield, based on $OsCl_4P_2$ used. The photochemical route from OsH_4P_3 is essentially quantitative, and the liberated phosphine can be removed in vacuo. The method thus provides an attractive high-yield synthesis of OsH_6P_2. Second, the implication of eq 3 is the unexpected one that OsH_4P_3 also undergoes photodissociation of PMe_2Ph. Equations 2 and 3 thus constitute the first documented example of a polyhydride that extrudes both H_2 and phosphine with comparable efficiencies. Any search to identify a single primary photoprocess is thus an oversimplification.

Relative Quantum Yield for H_2 and PMe_2Ph Loss. Competition experiments were used to determine the relative importance of the two photoprocesses. A solution of 0.03 M OsH_4P_3 in THF was divided in half; to one half (A) was added 0.15 M PMe_2Ph, and to the other (B) was added 0.15 M PEt_3. These solutions were irradiated side by side (254-nm monochromatic source) on a merry-go-round apparatus for 1 h. After irradiation, the disappearance (vide infra for products) of OsH_4P_3 was quantitated by $^{31}P\{^1H\}$ NMR spectroscopy, integration being with reference to a sealed tube of aqueous H_3PO_4 held coaxially in the NMR tubes. In the PMe_2Ph sample (A), conversion to *cis*-OsH_2P_4 occurred according to eq 2. The quantum yield for disappearance of OsH_4P_3 is simply related to the efficiency of photochemical H_2 loss, since the phosphine-loss pathway is totally inhibited by the added excess PMe_2Ph. In the PEt_3 solution (B), both phototransients are scavenged by added PEt_3 and both paths lead to depletion of OsH_4P_3 (eq 4, P = PMe_2Ph, P′ = PEt_3). Thus, in solution B the quantum yield for OsH_4P_3

$$\begin{array}{ccc} OsH_4P_3 & \xrightarrow[h\nu]{\Phi(H_2)} & OsH_2P_3 + H_2 \\ {\scriptstyle h\nu}\downarrow{\scriptstyle \Phi(P)} & & \downarrow{\scriptstyle P'} \\ & & OsH_2P_3P' \\ OsH_4P_2 + P & \xrightarrow{P'} & OsH_4P_2P' \end{array} \qquad (4)$$

loss is related to *both* H_2 and PMe_2Ph loss. In this latter case (B), OsH_4P_3 was lost nearly 3 times more efficiently than in the PMe_2Ph reaction, these conversions being expressed in eq 5. In a control experiment, a similar

$$\frac{\text{loss for B}}{\text{loss for A}} = \frac{\Phi(P) + \Phi(H_2)}{\Phi(H_2)} = 2.7 \qquad (5)$$

solution of $OsH_4(PMe_2Ph)_3$ and PEt_3 showed no thermal reaction after several hours at room temperature. From these relative quantum yields for OsH_4P_3 depletion, we can calculate that PMe_2Ph loss from OsH_4P_3 is 1.7 times more efficient than H_2 loss. Further, any explanation of photoreactivity (vide infra) must consider both OsH_2P_3 and OsH_4P_2 as available reactive intermediates.

OsH/C–D Exchange. Another "quenching" study attests to the high reactivity of the unsaturated OsH_xP_y transients. If the photolysis of OsH_4P_3 is carried out in C_6D_6 (under N_2), the ^1H NMR spectrum shows evidence of increasing amounts of C_6D_5H; likewise, unreacted OsH_4P_3 shows a loss of integrated intensity for Os–H relative to P–CH_3. Thus, one or both of the intermediates are capable of activating the aromatic C–D bonds and the exchange of Os–H for Os–D is 90% complete after 1 h of irradiation. In reactions of OsH_4P_3 to be discussed below (i.e. those executed in C_6D_6), solvent-derived deuterium is found in the ultimate photoproducts. Thus, H/D exchange of one or both primary photoproducts with aromatic solvents is more readily effected than are the subsequent processes.

Influence of the Coordinated Phosphine. In order to establish the extent to which the photochemistry is determined by the R groups on the phosphine, we investigated the photolysis of $OsH_4(PEt_3)_3$. Irradiation (through quartz apparatus) of $OsH_4(PEt_3)_3$ in either THF or benzene for 4–6 h gave (^{31}P NMR) no consumption of the tetrahydride; no solid is produced during this time. If 3 equiv of PEt_3 is added to $OsH_4(PEt_3)_3$ in either solvent, irradiation for 5 h likewise gives no conversion of tetrahydride. There is no formation of solid and no visual color change. Thus, $OsH_2(PEt_3)_4$ is not produced, and photodissociation of H_2 is ruled out.

The compound is photostable,[10] but it is not photoinert.[11] Irradiation of $OsH_4(PEt_3)_3$ under 60 atm of H_2 yields $OsH_6(PEt_3)_2$ (and equimolar PEt_3). Thus, for $OsH_4(PEt_3)_3$, phosphine photodissociation is the only detectable consequence of irradiation. However, no dimerization ensues from the transient $OsH_4(PEt_3)_2$. This transient does effect OsH/C_6D_6 exchange, however. Photolysis of $OsH_4(PEt_3)_3$ in C_6D_6 leads to 50% loss of OsH ^1H NMR intensity in 2 h; no deuterium is incorporated into the ethyl groups. We confirmed that $OsH_4(PEt_3)_2$ is responsible for this attack on solvent benzene by perceptibly reducing the rate of exchange during irradiation in the presence of 3.7 equiv of added PEt_3 and by

(10) That is, there is no net change from irradiation.
(11) That is, the excited state does decay by bond rupture.

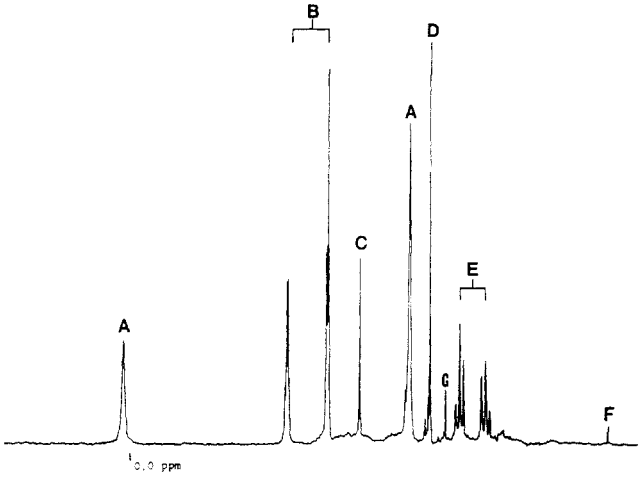

Figure 1. $^{31}P\{^1H\}$ NMR spectrum after photolysis of a saturated solution of OsH_4P_3 in THF: (A) $Os_2H_4P_6$; (B) $Os_2H_4P_5$; (C) $Os_2H_3P_6^+$; (D) OsH_4P_3; (E) *cis*-OsH_2P_4; (F) PMe_2Ph; (G) OsH_6P_2.

halting exchange altogether with 15 equiv of PEt_3.

Photochemistry in the Absence of Scavengers. A saturated solution of OsH_4P_3 in THF was irradiated for ca. 2 h in an NMR tube. At this time, the reaction was monitored by $^{31}P\{^1H\}$ NMR spectroscopy and the resultant spectrum is shown in Figure 1. In this complex spectrum, peak D (at −28.8 ppm) is due to unreacted OsH_4P_3. Peak F is free PMe_2Ph, the origin of which will be discussed below. The remaining products were identified by a combination of spectral and structural methods, and the assignments are discussed individually below.

OsH_6P_2 and *cis*-OsH_2P_4. These compounds were discussed above in connection with the trapping experiments involving H_2 and PMe_2Ph, respectively. Both are found in small amounts, even when the photochemistry is performed without added scavengers. The compound OsH_6P_2 gives rise to the singlet peak G in Figure 1 (−29.9 ppm); the corresponding ^1H NMR data for this hexahydride are given in the Experimental Section. This compound is rapidly fluxional on the NMR time scale, and we have been unable to freeze out this process at −70 °C in THF. However, the structure of $OsH_6(P^iPr_2Ph)_2$ has been determined[12] to be an OsH_6P_2 dodecahedron with the phosphines in the relatively unencumbered B sites.

The presence of stereochemically rigid *cis*-OsH_2P_4 is indicated by the $^{31}P\{^1H\}$ NMR A_2B_2 pattern of two triplets (labeled E in Figure 1). The hydride region of the ^1H NMR spectrum of *cis*-OsH_2P_4 is also quite characteristic due to the magnetic inequivalence of the two PMe_2Ph groups trans to hydride ligands; this spectrum has been discussed previously.[7]

$Os_2H_4P_6$ (3). This dimeric species (A in Figure 1) results from the photolysis of OsH_4P_3 in saturated benzene or THF solutions. Since **3** is only sparingly soluble, red crystals are deposited on the reactor walls. The crystal structure of compound **3** permitted the location of all four hydride ligands. As shown in Figure 2, the dimer consists of two edge-shared octahedra in which two *fac*-OsH_3P_3 centers share a $(\mu\text{-H})_2$ edge. The centrosymmetric structure is analogous to that assumed by $Ru_2H_4(PMe_3)_6$, which was prepared via a circuitous route from $Ru_2(\mu\text{-}CH_2)_3(PMe_3)_6$.[13]

(12) Howard, J. A.; Johnson, O.; Koetzle, T. F.; Spencer, J. L. *Inorg. Chem.* **1987**, *26*, 2930.

(13) Jones, R. A.; Wilkinson, G.; Colquohoun, I. J.; McFarlane, W.; Galas, A. M. R.; Hursthouse, M. B. *J. Chem. Soc., Dalton Trans.* **1980**, 2480.

Table I. Crystallographic Data

	$Os_2(H)_4(PMe_2Ph)_6$		
chem formula	$C_{48}H_{70}P_6Os_2$	space group	$P2_1/a$
a, Å	11.809 (5)	T, °C	−165
b, Å	18.355 (9)	λ, Å	0.71069
c, Å	12.494 (6)	ρ_{calcd}, g/cm^3	1.665
β, deg	116.64 (2)	μ(Mo K$_\alpha$), cm^{-1}	54.76
V, Å^3	2420.54	R	0.0468
Z	2	R_w	0.0412
fw	1213.32		
	$Os_2(H)_4(PMePh_2)_5$		
chem formula	$C_{65}H_{69}P_5Os_2$	space group	$P2_1/c$
a, Å	11.180 (5)	T, °C	−162
b, Å	22.161 (11)	γ, Å	0.71069
c, Å	25.098 (14)	ρ_{calcd}, g/cm^3	1.605
β, deg	112.79 (2)	μ(Mo K$_\alpha$), cm^{-1}	46.09
V, Å^3	5732.47	R	0.0496
Z	4	R_w	0.0485
fw	1385.53		
	$[Os_2(H)_3(PMe_2Ph)_6^+][Os(H)_4(PMe_2Ph)_2^-]$		
chem formula	$Os_3P_8C_{64}H_{107}$	space group	$C2/c$
a, Å	21.243 (12)	T, °C	−165
b, Å	12.366 (5)	γ, Å	0.71069
c, Å	25.676 (16)	ρ_{calcd}, g/cm^3	1.662
β, deg	96.97 (3)	μ(Mo K$_\alpha$), cm^{-1}	59.10
V, Å^3	6694.89	R	0.0461
Z	4	R_w	0.0428
fw	1674.78		
	$Os_2(H)_4(PMe_2Ph)_4(PMePh)_2$		
chem formula	$C_{46}H_{64}P_6Os_2$	space group	$P2_1/c$
a, Å	12.518 (3)	T, °C	−165
b, Å	12.026 (2)	λ, Å	0.71069
c, Å	16.484 (4)	ρ_{calcd}, g/cm^3	1.715
β, deg	112.59 (1)	μ(Mo K$_\alpha$), cm^{-1}	57.84
V, Å^3	2291.07	R	0.0425
Z	2	R_w	0.0407
fw	1183.25		

Table II. Selected Bond Distances (Å) and Angles (deg) for $Os_2H_4(PMe_2Ph)_6$

Os(1)-Os(1)′	2.818 (1)	Os(1)-H(1)	1.61 (9)
Os(1)-P(2)	2.261 (3)	Os(1)-H(2)	1.59 (10)
Os(1)-P(3)	2.257 (3)	Os(1)-H(2)′	2.18 (10)
Os(1)-P(4)	2.340 (3)		

Os(1)′-Os(1)-P(2)	130.2 (1)	P(2)-Os(1)-H(1)	87 (3)
Os(1)′-Os(1)-P(3)	132.7 (1)	P(2)-Os(1)-H(2)	171 (4)
Os(1)′-Os(1)-P(4)	92.2 (1)	P(3)-Os(1)-H(1)	81 (3)
P(2)-Os(1)-P(3)	94.4 (1)	P(3)-Os(1)-H(2)	83 (4)
P(2)-Os(1)-P(4)	100.2 (1)	P(4)-Os(1)-H(1)	172 (3)
P(3)-Os(1)-P(4)	94.5 (1)	P(4)-Os(1)-H(2)	94 (3)
Os(1)′-Os(1)-H(1)	86 (3)	H(1)-Os(1)-H(2)	89 (4)
Os(1)′-Os(1)-H(2)	34 (3)	H(2)-Os(1)-H(2)′	84 (5)

Selected bond lengths and angles for **3** are given in Table II. The formulation of an Os=Os double bond is required to give each osmium center an 18-electron count if two μ_2-hydrides donate a total of two electrons. The Os=Os distance is 2.818 (1) Å, which is virtually identical with the Ru=Ru distance (2.811 (4) Å) in $Ru_2H_4(PMe_3)_6$.[13] This distance is influenced by the presence of the bridging hydrogens that flank the metal–metal bond. In **3**, the bridging hydrides are refined to positions that are not equidistant from the metal centers. We feel this asymmetry is not real but rather an artifact due to the proximity of a 5d (i.e., heavy) metal scattering center. This is most clearly evident in the *equality* of the Os–P(2) and Os–P(3) distances, which should be unequal if the hydride bridges were truly asymmetric.

The coordination geometry around osmium approaches that of an octahedron, with the expected distortions arising from the facial array of bulky phosphines. The cis P–Os–P angles range from 94.4 (1) to 100.2 (1)°, the largest distortion arising in the P(2)–Os–P(4) angle. The Os–P bond

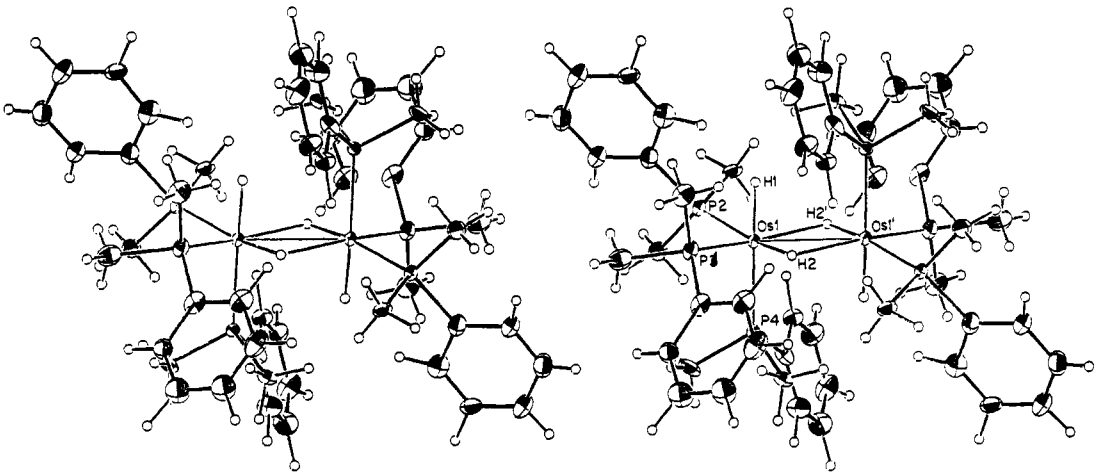

Figure 2. Stereo ORTEP drawing of $Os_2H_4(PMe_2Ph)_6$, showing selected atom labeling. Unlabeled P and H are related to those labeled by a center of symmetry.

lengths reflect the greater trans influence of the terminal hydride relative to that of the bridging hydrides: the axial phosphine (trans to terminal H(1)) shows an Os–P distance of 2.340 (3) Å, while the equatorial phosphines show Os–P distances of 2.257 (3) and 2.261 (3) Å. This corresponds to a difference of 19σ(diff) between the axial and equatorial Os–P bond lengths.

The $^{31}P\{^1H\}$ spectrum of **3** is consistent with the solid-state structure. It consists of two signals (labeled A in Figure 1) at 0.6 and −26.7 ppm, in an approximate 1:2 intensity ratio. While these signals are broadened, J_{PP} is not resolved.[14] However, the ^1H NMR spectrum is less clear-cut. The two types of P–CH_3 groups are evident at 1.70 and 1.48 ppm (1:2 ratio), but only one hydride signal (a broad multiplet at −13.6 ppm) is observed.[15]

$Os_2H_4(PMe_2Ph)_5$ (4). In contrast to the above results in THF or benzene, photolysis of a saturated ethanol solution of $OsH_4(PMe_2Ph)_3$ led to the deposition of *orange* crystals. These crystals were taken up in benzene, and the $^{31}P\{^1H\}$ NMR spectrum showed signals for compound **3** as well as those of an A_2X_3 system and of free PMe_2Ph. The A_2X_3 pattern of **4** is labeled B in Figure 1 and consists of a triplet at −19.0 ppm and a quartet at −14.7 ppm (J_{PP} = 5 Hz). Three separate efforts to crystallize **4** gave crystals that were shown by cell constant measurements to be $Os_2H_4P_6$ (**3**). If free PMe_2Ph is added to the mixture of **3** and **4**, the result is complete conversion to **3**. Conversely, if the solution is heated to 80 °C and all volatiles are removed in vacuo, the sample dissolves to give a mixture in which the proportion of **4** is dramatically increased. These observations are consistent with an equilibrium between **3** and **4**, as shown in eq 6. We estimate K_{eq} for

$$\underset{\mathbf{3}}{Os_2H_4P_6} \rightleftarrows \underset{\mathbf{4}}{Os_2H_4P_5} + P \qquad (6)$$

eq 6 is ca. 2–4 mol/L, and it remains constant in THF, benzene, and acetonitrile solutions. The kinetics of this process are such that rapid (minutes) equilibration occurs only at elevated temperatures. If the equilibrium (eq 6) is pushed to the right at 80 °C and then the solution cooled immediately to 25 °C, the original (25 °C) equilibrium concentrations are restored only after ca. 24 h.

The phosphine dissociation equilibrium (eq 6) leads to the conclusion that $Os_2H_4P_5$ is the formula of **4**, and the presence of five PMe_2Ph ligands is consistent with the A_2X_3 pattern in the $^{31}P\{^1H\}$ spectrum. When coupling is permitted to only the (upfield) hydrides, the ^{31}P NMR A_2X_3 signals are converted to multiplets. The ^1H NMR spectrum shows two types of PMe doublets that overlap at 1.88 ppm and an additional PMe doublet at 1.47 ppm. The overlapping doublets are indicative of diastereotopic methyl groups, consistent with the presence of a mirror plane. The hydride region contains a broad pseudodoublet at −8.95 ppm and a triplet at −19.81 ppm (J = 27 Hz), with integrated intensities in a ratio of ca. 3:1. These data are consistent with a face-shared octahedral structure, $HP_2Os(\mu\text{-}H)_3OsP_3$, for **4**. We sought structural verification of this, but the presence of traces of **3** precluded clean crystallization of **4**. To circumvent this, we sought an analogue of **4** with a bulkier phosphine, hoping to enhance ligand dissociation. Indeed, photolysis of $OsH_4(PMePh_2)_3$ proceeds with exclusive formation of $Os_2H_4(PMePh_2)_5$ (**5**; eq 7). The spectral data for **5** (see Experimental Section) are sufficiently similar to those of **4** that it is probable that the compounds are isostructural.

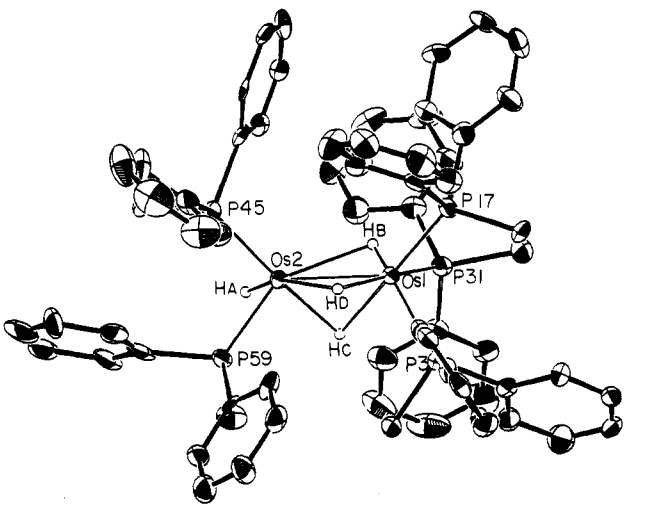

Figure 3. ORTEP drawing of $Os_2H_4(PMePh_2)_5$, showing selected atom labeling.

$$2OsH_4(PMePh_2)_3 \xrightarrow[THF]{h\nu} \underset{\mathbf{5}}{Os_2H_4(PMePh_2)_5} + PMePh_2 + 2H_2 \qquad (7)$$

Red-orange crystals of **5** were obtained from toluene/acetonitrile. The structure is shown in Figure 3, with

(14) The less intense signal is broader, suggesting unresolved triplet structure.

(15) An upfield hydride resonance could be not identified with certainity due to low solubility and resultant poor signal-to-noise ratio.

Table III. Selected Bond Distances (Å) and Angles (deg) for $Os_2H_4(PMePh_2)_5$

Os(1)-Os(2)	2.551 (1)	Os(1)-P(31)	2.295 (3)
Os(1)-P(3)	2.297 (3)	Os(2)-P(45)	2.236 (3)
Os(1)-P(17)	2.311 (3)	Os(2)-P(59)	2.230 (3)
Os(2)-Os(1)-P(3)	116.3 (1)	P(17)-Os(1)-P(31)	95.3 (1)
Os(2)-Os(1)-P(17)	127.4 (1)	Os(1)-Os(2)-P(45)	130.6 (1)
Os(2)-Os(1)-P(31)	117.4 (1)	Os(1)-Os(2)-P(59)	127.3 (1)
P(3)-Os(1)-P(17)	97.0 (1)	P(45)-Os(2)-P(59)	95.9 (1)
P(3)-Os(1)-P(31)	97.5 (1)		
Os(1)-H(B)	1.11	Os(2)-H(D)	2.19
Os(1)-H(D)	2.01	Os(2)-H(C)	2.27
Os(1)-H(C)	2.27	Os(2)-H(B)	2.36
Os(2)-H(A)	1.77		
H(B)-Os(1)-H(D)	114	H(A)-Os(2)-H(C)	70
H(B)-Os(1)-H(C)	75	H(A)-Os(2)-H(B)	102
H(B)-Os(1)-P(31)	63	H(A)-Os(2)-Os(1)	119
H(B)-Os(1)-P(3)	156	H(D)-Os(2)-P(59)	99
H(B)-Os(1)-P(17)	98	H(D)-Os(2)-P(45)	108
H(B)-Os(1)-Os(2)	67	H(D)-Os(2)-H(C)	91
H(D)-Os(1)-H(C)	96	H(D)-Os(2)-H(B)	72
H(D)-Os(1)-P(31)	172	H(D)-Os(2)-Os(1)	49
H(D)-Os(1)-P(3)	84	P(59)-Os(2)-H(C)	91
H(D)-Os(1)-P(17)	92	P(59)-Os(2)-H(B)	147
H(D)-Os(1)-Os(2)	56	P(45)-Os(2)-H(C)	158
H(C)-Os(1)-P(31)	76	P(45)-Os(2)-H(B)	117
H(C)-Os(1)-P(3)	88	H(C)-Os(2)-H(B)	58
H(C)-Os(1)-P(17)	171	H(C)-Os(2)-Os(1)	56
H(C)-Os(1)-Os(2)	56	H(B)-Os(2)-Os(1)	26
H(A)-Os(2)-H(D)	161	Os(1)-H(B)-Os(2)	87
H(A)-Os(2)-P(59)	76	Os(1)-H(C)-Os(2)	68
H(A)-Os(2)-P(45)	91	Os(1)-H(D)-Os(2)	75

selected bond lengths and angles in Table III. The dimer is an unsymmetrical confacial bioctahedron composed of OsP_3 and $OsHP_2$ fragments sharing a common $(\mu\text{-H})_3$ face. Both osmium centers show distortions from octahedral geometry due to repulsions between $PMePh_2$ moieties, but the nature of these distortions is different at the two metal centers. Crowding is not apparent from a comparison of P–Os–P angles: for the *fac*-OsP_3 center, these angles average 96.6°, and for the $OsHP_2$ center, the P–Os–P angle is 95.9 (1)°. However, the relative steric demands are indicated by two other criteria. In the *fac*-OsP_3 center, the Os–P bond lengths average 2.301 Å, and in the $OsHP_2$ center, they average 2.233 Å, a difference of 0.068 Å or 16σ(diff). Also, the Os–Os–P angles reflect an encroachment of the two phosphines on the terminal hydride at Os(2); Os2–Os1–P angles are 116.3 (1), 127.4 (1), and 117.4 (1)°, while Os(1)–Os(2)–P angles are 127.3 (1) and 130.6 (1)°.

An 18-electron count at both osmium centers requires an Os–Os triple bond (assuming one electron donated by each μ-hydride). The observed bond length is 2.551 (1) Å, or 0.27 Å shorter than the Os=Os double bond in $Os_2H_4P_6$ (**3**).

A difference Fourier peak assigned as a terminal hydride (H_A) is found 1.77 Å from Os(2). Terminal Os–H distances determined by neutron diffraction studies on $OsH_4(PMe_2Ph)_3$ average 1.659 (3) Å. Peaks considered as possible μ-hydrides show Os–H distances ranging from 1.11 to 2.36 Å; these are clearly incorrect due to the presence of other residuals in the Os_2 internuclear region. These hydrides are included in Figure 3 primarily to display the face-shared octahedral character of the structure.

In a comparison of the solid-state structure with the NMR data for **5**, it becomes clear that the NMR data show less complexity than would be expected. This is most obvious from the A_2X_3 pattern in the $^{31}P\{^1H\}$ spectrum; while there exists idealized mirror symmetry, there is no 3-fold axis to equate the OsP_3 phosphines or the three bridging hydrides. We employed selective-decoupling experiments to further explore this paradox. If the ^{31}P signal for the $OsHP_2$ phosphines (6.2 ppm) is irradiated, the result is loss of triplet structure in the ^{31}P signal at −1.9 ppm, as well as loss of triplet structure for the terminal hydride H_A (−20.1 ppm). This experiment has no detectable effect on the $(\mu\text{-H})_3$ doublet at −8.9 ppm. Conversely, if the ^{31}P signal for the OsP_3 phosphines (−1.9 ppm) is irradiated, the result is loss of quartet structure in the ^{31}P signal at 6.2 ppm, as well as collapse of the $(\mu\text{-H})_3$ signal at −8.9 ppm to a singlet. The hydride triplet at −20.1 ppm remains unaffected. These results are reinforced by the observation that hydride coupling of the ^{31}P NMR spectrum doubles the multiplets seen at −1.9 and 6.2 ppm. These results show that the signal for terminal hydride H_A derives its triplet structure from coupling to two cis phosphines and that coupling of terminal H_A to bridging hydrides is unresolvably small. Similarly, the bridging hydrides couple only to the OsP_3 phosphines and not to the phosphines in the $OsHP_2$ fragment. All of these data can be accommodated by the *fluxional process*

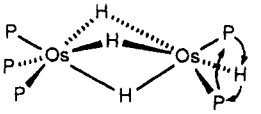

Here, the dimer can be thought of as containing a rigid *fac*-P_3OsH_3 center connected to an $OsHP_2$ center. The latter spins about the metal–metal bond axis, with the $(\mu\text{-H})_3$ face rigid. Thus, coupling of P and hydride nuclei in the $OsHP_2$ unit to the bridging hydrides is averaged to ca. zero, even though an average end-to-end P–P coupling (6 Hz) is maintained. The μ-hydride signal is a doublet due to dominant coupling to the single trans phosphorus in the rigid *fac*-P_3OsH_3 unit. This type of rotational motion has been previously observed, even in systems spanned by bridging ligands. Note that the observation of diastereotopic ortho phenyl proton resonances rules out the "inversion" motion of the $OsHP_2$ moiety shown in eq 8.

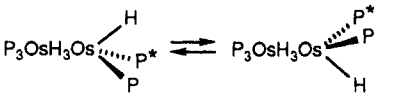

(8)

Knowledge of the structures of both **3** and **4** (by analogy to **5**) allow a detailed description of their equilibrium interconversion. This is represented in eq 9. The terminal

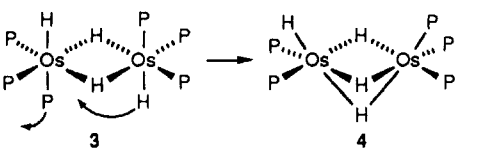

(9)

3 **4**

hydride in **3** serves to labilize the axial phosphine; as this phosphine leaves, the terminal hydride on the opposite osmium center swings into a bridging position, filling the site of unsaturation. Clearly, the steric bulk of the phosphine exerts substantial control over the equilibrium in eqs 6 and 9. In the system with PMe_2Ph, compounds **3** and **4** are both accessible. With bulkier $PMePh_2$, the equilibrium lies far to the right; we find that even large excesses of added $PMePh_2$ fail to convert **5** to $Os_2H_4(PMePh_2)_6$. Interestingly, if excess PMe_2Ph is added to a THF solution of $OsH(PMePh_2)_2(\mu\text{-H})_3Os(PMePh_2)_3$ (**5**), $^{31}P\{^1H\}$ NMR spectroscopy shows facile conversion (20 h, 25 °C) to $Os_2H_4(PMe_2Ph)_6$ (**3**) and free $PMePh_2$. This is indicative of incipient coordinative unsaturation in the $Os_2H_4P_5$ species.

$Os_2H_3P_6^+X^-$ (6). When OsH_4P_3 is photolyzed in *dilute* benzene solution, the result is precipitation of a yellow crystalline compound, **6**. This compound exhibits extremely low solubility in both aromatic solvents and THF. It dissolves slightly in acetonitrile and ethanol and shows substantial solubility in methylene chloride. The $^{31}P\{^1H\}$ NMR spectrum (in CH_2Cl_2) showed a singlet at −21.9 ppm (resonance C in Figure 1, which is supersaturated with **6**); coupling to upfield (hydride) resonances in the ^1H spectrum converted the ^{31}P singlet to a doublet, suggesting each phosphorus couples strongly only to one (trans) hydride in a nonfluxional structure. The ^1H NMR spectrum in CD_2Cl_2 showed P–Ph resonances as well as one P–Me signal (1.62 ppm) and a broad Os–H signal at −9.45 ppm. The simplicity of these spectra suggests a highly symmetrical molecule. In seeking a method of identifying the species responsible for these spectra, we were led to attempt the acidolysis of $Os_2H_4P_6$ (**3**) based on similar chemistry reported for a ruthenium analogue.[13] The reaction proceeds as in eq 10, leading to a cationic dimer

$$\underset{\mathbf{3}}{Os_2H_4P_6} + HBF_4{\cdot}Et_2O \rightarrow [Os_2H_3P_6][BF_4] + H_2 \qquad (10)$$

whose ^{31}P and ^1H NMR spectra were identical with those of the isolated yellow photoproduct (**6**). We also sought X-ray verification of the dimeric structure, as well as an identification of the counterion. Since crystals of **6** formed during photolysis were not suitable for diffraction, compound **6** was recrystallized from CH_2Cl_2/THF. From the X-ray study, the cation was clearly characterized as $P_3Os(\mu\text{-}H)_3OsP_3^+$;[8] however, the counterion in this recrystallized material was chloride. This evidently originated from the CH_2Cl_2 used in recrystallization, apparently by reaction of CH_2Cl_2 with the anion originally present in **6**.

The foregoing information raised questions regarding the nature of the "NMR-silent" anion in the photolysis product, as well as the mode of formation of an ionic salt in benzene solvent. To test for the participation of adventitious hydroxyl groups (i.e., deprotonation of a hydride as a source of anionic and cationic species), the photolysis was performed in benzene to which a few microliters of H_2O had been added. This had no obvious effect on the production of the salt **6**. In another experiment, all glassware was treated with a commercial silylating reagent[16] to remove surface hydroxyl groups; this had no effect on the production of **6**.

Due to the reaction with CH_2Cl_2, it was necessary to identify **6** without exposure to chlorocarbon solvents. An obvious means to test the reactivity of various solvents was a comparison of the IR spectra of the yellow solid before and after dissolution. This test revealed that the isolated photoproduct **6** exhibited a very strong and broad IR absorption at 1820 cm^{-1}, which was lost upon treatment with CH_2Cl_2. The absorption is in a position typical of terminal metal hydrides (yet the cation $Os_2H_3P_6^+$ has none). Moreover, the acidolysis product $[Os_2H_3P_6][BF_4]$ in eq 10 did not exhibit the 1820-cm^{-1} band. This suggested that the anion was an osmium species containig terminal hydrides. However, even though IR studies showed this presumed anion stable to solvents such as THF and acetonitrile, ^1H and ^{31}P NMR spectra in these solvents showed no evidence of resonances due to the anion. Further evidence for the Os–H assignment was obtained by performing the photolysis in C_6D_6. This led to a decrease in the intensity of the absorption at 1820 cm^{-1}, indicating substitution of Os–D for Os–H in the anion (recall that OsH_4P_3 undergoes facile H/D exchange in C_6D_6 faster than its subsequent photochemistry). The band at 1820 cm^{-1} is thereby confirmed to be due to a hydride motion.

(16) $Cl(Me_2SiO)_4Cl$, sold as "Surfasil" by Pierce Chemical Co.

Table IV. Selected Bond Distances (Å) and Angles (deg) for $[Os_2H_3(PMe_2Ph)_6][OsH_x(PMe_2Ph)_2]$

Os(1)–Os(1)′	2.558 (2)	Os(2)–P(6)	2.267 (3)
Os(1)–P(3)	2.286 (3)	Os(1)–H(1)	1.95 (10)
Os(1)–P(4)	2.296 (3)	Os(1)–H(2)	1.63 (16)
Os(1)–P(5)	2.292 (3)		
Os(1)′–Os(1)–P(3)	124.5 (1)	P(3)–Os(1)–H(1)	94 (2)
Os(1)′–Os(1)–P(4)	123.9 (1)	P(4)–Os(1)–H(1)	173 (2)
Os(1)′–Os(1)–P(5)	120.9 (1)	P(5)–Os(1)–H(1)	90 (2)
P(3)–Os(1)–P(4)	92.5 (1)	P(5)–Os(1)–H(2)	163 (5)
P(3)–Os(1)–P(5)	93.1 (1)	H(1)–Os(1)–H(2)	90 (6)
P(4)–Os(1)–P(5)	93.5 (1)		

The failure to observe the anion of **6** via NMR spectroscopy suggested that the species either was paramagnetic or was undergoing some exchange process which was rapid on the NMR time scale. Since we did not know, a priori, the ease of fluxionality of polyhydride anions, we sought examples to serve as potential models for the anion in **6**. The use of potassium hydride to deprotonate metal hydrides has been demonstrated.[17,18] When OsH_4P_3 is treated with KH in THF at 70 °C, K[*fac*-OsH_3P_3] forms quantitatively (eq 11). This compound exhibits ^1H and

$$OsH_4P_3 + KH \xrightarrow[THF]{} K[\textit{fac}\text{-}OsH_3P_3] + H_2 \qquad (11)$$

^{31}P NMR data expected for a stereochemically rigid AA′A″XX′X″ system, and the hydride resonance pattern is virtually identical with that of the isoelectronic *fac*-$IrH_3(PEt_2Ph)_3$.[19] The $OsH_3P_3^-$ anion is a very strong Brønsted base, and solvents and glassware must be rigorously dry to prevent reversion to OsH_4P_3, but it was obviously not the anion in compound **6**. The higher valent compound OsH_6P_2 can be similarly deprotonated, under milder conditions. This reaction (eq 12) proceeds immediately at room temperature, and the anion is considerably less basic and can be isolated as the potassium salt. The seven-coordinate anion $OsH_5P_2^-$ exhibits a $^{31}P\{^1H\}$ NMR singlet and a single binomial triplet for the hydride ligands. The $^{31}P\{^1H\}$ NMR spectrum (40.5 MHz) is unchanged to −85 °C. These data are consistent with a pentagonal-bipyramidal structure with axial phosphines, as was reported[20] for the isoelectronic $IrH_5(P^iPr_3)_2$. In summary, then, these particular $OsH_xP_z^-$ systems show perfectly reasonable NMR data and certainly neither *is* the anion in **6**. The anion in **6** must therefore be paramagnetic.

$$OsH_6P_2 + KH \xrightarrow[THF]{} K[OsH_5P_2] + H_2 \qquad (12)$$

Since the crystals produced by conventional direct irradiation were too small for X-ray diffraction, we sought to slow the production and precipitation of **6**, a task accomplished by moving the solution some distance from the lamp (effectively lowering the light intensity). The X-ray structure determined from crystals obtained in this manner is illustrated in Figure 4, and bond lengths and angles are given in Table IV. The structure confirms the presence of the cation $Os_2H_3P_6^+$, whose determined structure is indistinguishable from that reported previously for $[Os_2$-

(17) Huffman, J. C.; Green, M. A.; Kaiser, S. L.; Caulton, K. G. *J. Am. Chem. Soc.* **1985**, *107*, 5111.
(18) Alvarez, D.; Lundquist, E. G.; Ziller, J. W.; Evans, W. J.; Caulton, K. G. *J. Am. Chem. Soc.* **1989**, *111*, 8392.
(19) *Transition Metal Hydrides*; Muetterties, E. L., Ed.; Dekker: New York 1971; p 80.
(20) Garlaschelli, L.; Khan, S. I.; Bau, R.; Longoni, G.; Koetzle, T. F. *J. Am. Chem. Soc.* **1985**, *107*, 7212.

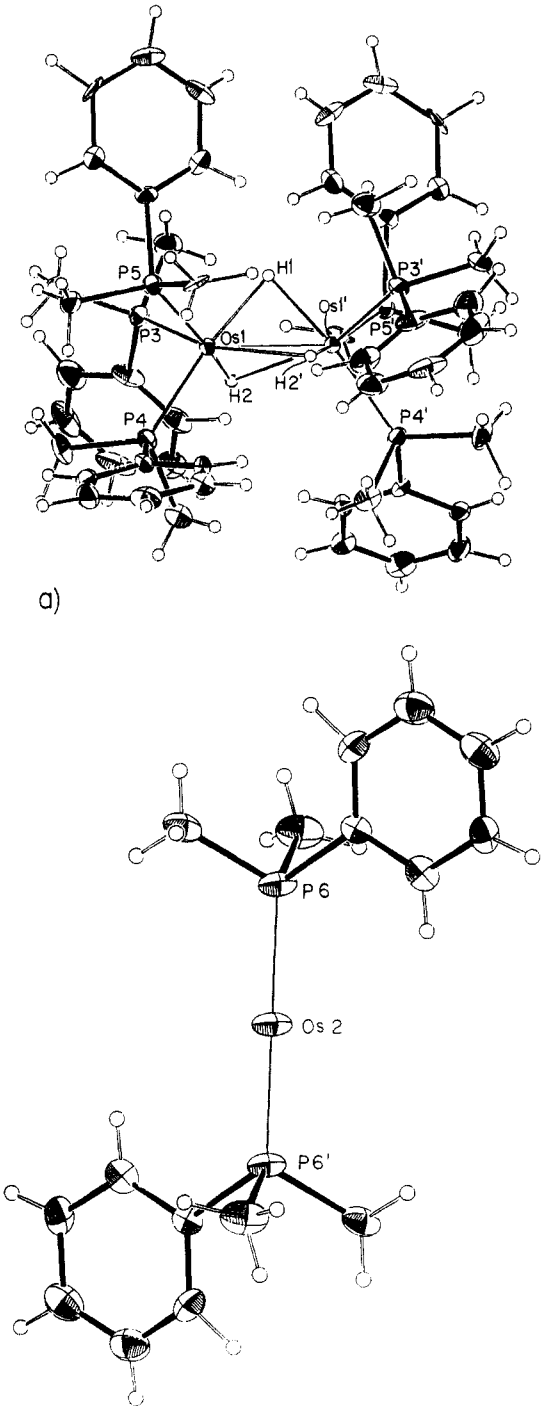

Figure 4. ORTEP drawings and selected atom labeling of (a) $Os_2H_3(PMe_2Ph)_6^+$ and (b) $OsH_4(PMe_2Ph)_2^-$ in their 1:1 salt.

$H_3P_6]Cl$,[8] with the exception of the refined positions of the bridging hydrides. The cation is composed of two octahedral *fac*-H_3OsP_3 centers sharing a (μ-H)$_3$ face. The ends of the molecule are related by a crystallographic C_2 axis passing through H(1) and the Os–Os midpoint. The three independently determined P–Os–P angles average 93.1 (1)°, reflecting a slight expansion from a perfect octahedral geometry. The Os–P bond lengths average 2.291 (3) Å, and the Os–Os–P angles average 123.1 (1)°. As in $HP'_2Os(\mu\text{-}H)_3OsP'_3$ (**5**), the electron count in $Os_2H_3P_6^+$ requires a triple Os–Os bond and the bond distances in these compounds (**5** and **6**) are identical at 2.558 (2) Å.

The hydride positions refined from X-ray data show a great deal of asymmetry in the cation of **6**, particularly when compared to those in $[Os_2H_3P_6]Cl$. In the latter compound, the hydrides were refined to positions equidistant from the two metals within 3σ.[8] In the structure of **6**, only H(1) was refined to a position equidistant from the two metals in the dimer. The other hydride H(2) and H(2)′ was refined to a site (related by the crystallographic C_2 axis) 1.63 (16) Å from one metal and 2.55 (18) Å from the other. We conclude that the data confirm the *presence* of hydride ligands, but the structural parameters themselves suffer systematic error from residuals in the final difference map.

We now turn our attention to the counterion in **6**, the identification of which prompted this structural study. The X-ray study, by charge balance, definitively establishes the counterion charge as −1. As is evident in Figure 4, the anion is a monomer with a linear P–Os–P array lying on a crystallographic center of symmetry. Unfortunately, no electron density due to the hydrides could be detected in this anion, even though all carbon-bound hydrogens in both cation and anion were detected and refineable. The latter success speaks for the quality of the diffraction data set, and we conclude that the hydride ligands in the anion are disordered. We presume that these hydrides lie in the plane perpendicular to the P–Os–P axis and that the hydride positions fail to be refined due to disorder about this axis. Although disappointing, these results allow the formulation $OsH_nP_2^-$ for the anion, where n must be even to account for the paramagnetism (and hence the lack of ^1H and ^{31}P NMR signals) of the anion.

Since the anion $OsH_nP_2^-$ is paramagnetic, we sought to find a reagent to effect net transfer of one hydrogen *atom* to the anion, converting it to a diamagnetic species more suitable for characterization. Attempts in this vein involved treatment of $[Os_2H_3P_6][OsH_nP_2]$ (**6**) with either 2-propanol or 1,4-cyclohexadiene. Both of these reagents can serve as sources of hydrogen atoms, but neither exhibited any reaction with **6**. In a search for a better soruce of hydrogen atoms, advantage was taken of the tendency of tin hydrides toward hydrogen atom transfer.[21] Indeed, reaction of **6** with Bu_3SnH proceeded with hydrogen transfer to the paramagnetic anion (eq 13). The resulting

$$[Os_2H_3P_6][OsH_4P_2] + Bu_3SnH \rightarrow [Os_2H_3P_6][OsH_5P_2] + (Bu_3Sn)_2 \quad (13)$$

anion has a five-hydride count, which supports the identification of its predecessor as the 17-electron six-coordinate *trans*-$OsH_4P_2^-$. The diamagnetic anion produced in eq 13 was identical with that in $K[OsH_5P_2]$, described above from treatment of OsH_6P_2 with KH. The identity of **6** is particularly remarkable in view of the facile photochemical production of the paramagnetic anion. This is the first isolated monomeric odd-electron polyhydride species devoid of halide ligands.[22]

An effort to further test the Os(III) oxidation state assignment in the anion was made by using variable-temperature magnetic susceptibility measurements on $[Os_2H_3(PMe_2Ph)_6][OsH_4(PMe_2Ph)_2]$. A magnetic susceptibility of (5.5 (±1)) × 10^{-4} emu mol^{-1} was measured; this value was found to be *independent* of temperature within the signal-to-noise limits of the Faraday apparatus employed. An attempt was made to model this magnetic behavior by employing configuration interaction of t_{2g}^4e- and t_{2g}^5-derived states of Os(III); the model of Hill[23] includes as parameters the wave function mixing coefficients, a spin–orbit coupling constant, Racah and orbital reduction

(21) Kuivila, H. G. *Acc. Chem. Res.* **1968**, *1*, 299.
(22) For a transient paramagnetic example, see: Bruno, J. W.; Caulton, K. G. *J. Organomet. Chem.* **1986**, *315*, C13.
(23) Hill, N. J. *J. Chem. Soc., Faraday Trans. 2* **1972**, *68*, 427.

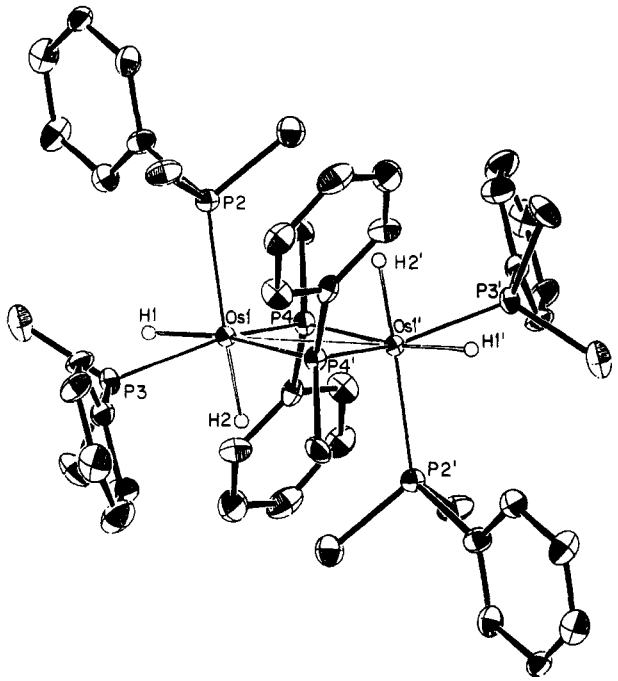

Figure 5. ORTEP drawing of $Os_2H_4(\mu\text{-PMePh})_2(PMe_2Ph)_4$, showing selected atom labeling. Unlabeled ellipses are carbon, and primed atoms are related to unprimed atoms by a center of symmetry.

parameters, and a state energy gap. An exploration of this parameter space revealed that, while the susceptibility is predicted to be temperature *dependent*, reasonable parameter values yield susceptibility values so small that they are on the order of the noise limits of our measurements on this high-molecular-weight material; unique sets of parameters could not be found. Thus, while it is not possible to definitively determine the number of unpaired electrons from susceptibility measurements, these results are not contradictory to the proposal of $OsH_4(PMe_2Ph)_2$ stoichiometry.

$Os_2H_4(PMePh)_2(PMe_2Ph)_4$ (7). The same benzene solution from which $[Os_2H_3(PMe_2Ph)_6][OsH_4(PMe_2Ph)_2]$ precipitates during prolonged photolysis of a dilute solution of $OsH_4(PMe_2Ph)_3$ also contains a soluble molecular product. This compound is not evident in Figure 1, since it is observed only after prolonged photolysis. The ^1H NMR spectrum of this compound contains only doublets in the P–Me region of the spectrum (suggesting no trans disposition of two phosphines), but there are *five* doublets of equal intensity, indicating low symmetry. The *odd* number (five) of resonances is particularly surprising. The compound contains two equally intense hydride resonances, one a broad triplet and the second a broad doublet. The $^{31}P\{^1H\}$ NMR spectrum exhibits three equally populated chemical shifts (hence, the molecule contains some multiple of three phosphorus nuclei), two of which show strong (117 Hz) mutual coupling and hence are probably of trans stereochemistry. One of the three ^{31}P chemical shifts is very far downfield (126.9 ppm).

Compound **7** was established to be $Os_2H_4(\mu\text{-PMePh})_2(PMe_2Ph)_4$ by X-ray crystallography. The structure of **7**, composed of two edge-shared octahedra, is illustrated in Figure 5, and bond lengths and angles are given in Table V. The dimer has a crystallographic center of symmetry, and therefore Os, Os′, P(4), and P(4)′ are rigorously coplanar, as are P(2), P(2)′, Os, and Os′; the angle between these two planes is 90.4°. In **7**, the bridging ligands are the phosphides (PMePh) and each osmium also bears two terminal cis hydrides and two cis phosphines. This accounts completely for the number of ^1H and ^{31}P chemical shifts observed. If the μ-PMePh groups are counted as three-electron donors, an Os–Os single bond is required to give each osmium 18 valence electrons. The metal–metal distance is 2.889 (1) Å, consistent with formulation as a single bond flanked by bridging phosphides. For comparison, the Ru=Ru double bond in $Ru_2(NO)_2(PMePh_2)_2(\mu\text{-PPh})_2$ is 2.629 (2) Å.[24] A distinctive downfield ^{31}P resonance (126.9 ppm) of the phosphide phosphorus in **7** is an empirical indication of the presence of a metal–metal bond.[25]

Table V. Selected Bond Distances (Å) and Angles (deg) for $Os_2(H)_4(PMe_2Ph)_4(PMePh)_2$

Os(1)–Os(1)′	2.889 (1)	Os(1)–P(4)′	2.325 (2)
Os(1)–P(2)	2.364 (2)	Os(1)–H(1)	1.48 (9)
Os(1)–P(3)	2.290 (2)	Os(1)–H(2)	1.56 (14)
Os(1)–P(4)	2.312 (2)		
Os(1)′–Os(1)–P(2)	101.1 (1)	Os(1)–Os(1)–H(1)	149 (4)
Os(1)′–Os(1)–P(3)	149.9 (1)	Os(1)–Os(1)–H(2)	77 (5)
Os(1)′–Os(1)–P(4)	51.7 (1)	P(2)–Os(1)–H(1)	86 (4)
P(2)–Os(1)–P(3)	98.4 (1)	P(2)–Os(1)–H(2)	171 (5)
P(2)–Os(1)–P(4)	97.2 (1)	P(3)–Os(1)–H(1)	55 (4)
P(3)–Os(1)–P(4)	104.0 (1)	P(4)–Os(1)–H(1)	159 (4)
P(4)–Os(1)–P(4)′	102.9 (1)	P(4)–Os(1)–H(2)	74 (5)
Os(1)–P(4)–Os(1)′	77.1 (1)	H(1)–Os(1)–H(2)	92 (6)

Scheme I

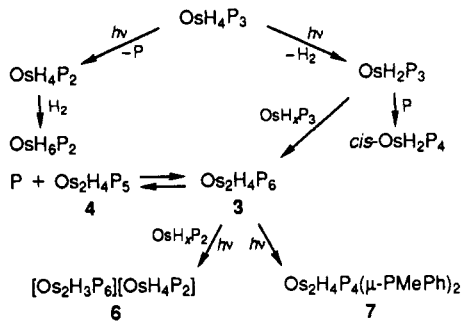

The Os–P distances for the μ-phosphide ligands (2.312 (2) and 2.325 (2) Å) are intermediate between those of the equatorial (2.290 (2) Å) and axial (2.364 (2) Å) phosphines. The latter distance reflects the trans influence of the terminal hydride H(2), and the asymmetry of the μ-PMePh position reflects a similar (but very small) influence exerted by H(1). The terminal hydrides were refined to distances (1.48 (9) and 1.56 (14) Å) that are within 2σ of the Os–H distance (1.659 (3) Å) obtained from neutron data previously discussed.[9] The Os–Os–P(2) angle (101.1 (1)°) indicates that the axial phosphine bends away from the congested center of the molecule toward the hydride H(1). This congestion is evident in Figure 5. While the Os–P(4)–Os′ angle is compressed to 77.1 (1)°, the C(methyl)–P(4)–C(phenyl) angle (98.9 (4)°) is not at all expanded compared to C–P–C angles in the other tertiary phosphine ligands (95.1 (5) and 100.9 (4)°).

Discussion

The formation of numerous products marks OsH_4P_3 as a compound with a rich and diverse photochemistry but also makes for a complex mechanistic picture. A reaction sequence to account for the observed products is presented in Scheme I. Major features include the presence of two primary photochemical events, H_2 loss and phosphine loss,

(24) Reed, J.; Schultz, A. J.; Pierpont, C. G.; Eisenberg, R. *Inorg. Chem.* **1973**, *12*, 2949.
(25) (a) Garrou, P. E. *Chem. Rev.* **1981**, *81*, 229. (b) Rosenberg, S.; Whittle, P. R.; Geoffroy, G. L. *J. Am. Chem. Soc.* **1984**, *106*, 5934.

as well as the identification of $Os_2H_4P_6$ (3) as a source of *secondary photochemistry*. The operation of two primary photoprocesses is clearly indicated by independent trapping studies with H_2 and with PMe_2Ph. While we can determine the relative primary efficiencies with which the transients OsH_2P_3 and OsH_4P_2 are produced, there is no obvious way of determining their efficiencies in subsequent reactions. One consideration is that OsH_4P_2 is produced by dissociation of liquid PMe_2Ph, which presumably remains available for nonproductive recombination. Conversely, OsH_2P_3 is derived from the loss of volatile H_2, which can be lost to the atmosphere under ambient conditions. We have noted that OsH_6P_2 is usually a minor photolysis product and that it arises from H_2 scavenging of OsH_4P_2; consistent with this view, the production of OsH_6P_2 is enhanced when carried out in a quartz tube (e.g. NMR tube) in which there is little headspace and inefficient transfer between the solution and gas phases.

We propose that $OsH_2(PMe_2Ph)_3$ is the unsaturated transient which leads to Os_2 products. In general terms, it is a well-established principle that unsaturated compounds may condense with hydride complexes to form hydride-bridged dimers.[26] More specifically, however, the idea that an osmium *di*hydride leads to Os_2 products follows from our studies of the photochemistry of $OsH_4(PEt_3)_3$. This molecule undergoes no net change upon photolysis (6 h) in THF or in C_6H_6. However, if the photoreaction is run under 1000 psi of H_2, the result is quantitative conversion to $OsH_6(PEt_3)_2$. Likewise, photolysis of $OsH_4(PEt_3)_3$ in C_6D_6 leads to facile H/D exchange, resulting in $Os(H/D)_4(PEt_3)_3$. In the presence of excess PEt_3 this exchange is inoperative, yet there is no conversion to *cis*-$OsH_2(PEt_3)_4$. These data suggest that, in contrast to the case for $OsH_4(PMe_2Ph)_3$, $OsH_4(PEt_3)_3$ undergoes exclusive photochemical loss of tertiary phosphine. The resultant $OsH_4(PEt_3)_2$ transient is capable of effecting H/D exchange, a process that is quenched when the intermediate is trapped by excess phosphine, yet *this OsH_4P_2 transient does not yield dimeric products*. The implication is that an Os(II) hydride is required to lead to dimeric polyhydrides.

Once formed, the Lewis acid OsH_2P_3 reacts with another polyhydride species (the donor) to yield $Os_2H_4P_6$ (3). The unidentified species OsH_xP_3 (Scheme I) could be either OsH_4P_3 or another OsH_2P_3, either of which has the requisite number of phosphines still ligated. We favor the former path, due to the low probability of collision of two transients (i.e. low concentration). This mechanism is consistent with flash photolytic studies on the dimerization of ReH_5P_3 to $Re_2H_8P_4$;[27] here the transient ReH_5P_2 was observed to react with the starting material ReH_5P_3 on the pathway to $Re_2H_8P_4$.

Conversion of two OsH_4P_3 molecules to one molecule of 3 involves the release of 2 equiv of H_2. Over time, the accumulated dissolved H_2 scavenges OsH_4P_2 to produce OsH_6P_2 (Figure 1). This explains the photochemical production of OsH_6P_2 in reaction mixtures to which no external H_2 was added.

The thermal equilibrium relating 3 and 4 has been observed directly and is undoubtedly the major source of 4 in the photochemistry. This equilibrium (3 $\rightleftharpoons$ 4) liberates phosphine, which can react with OsH_2P_3 to produce *cis*-OsH_2P_4 (Figure 1). Again, *cis*-OsH_2P_4 is a minor product that usually appears after some induction period, consistent with the sluggish kinetics and modest equilibrium constant for dissociation of 3 into 4 and PMe_2Ph.

The production of dimeric 3 is the key to the other dimeric products shown in Scheme I. The formation of compounds 6 and 7 can be demonstrated to arise from secondary photolysis of 3, but the actual mechanisms remain obscure. We have ruled out secondary photolysis of 4 because we have isolated 4 (after driving the 3 $\rightleftharpoons$ 4 equilibrium to 4 at high temperature) and found it to be photostable under typical reaction conditions. To study the photochemical behavior of 3, an equilibrium mixture of 3 and 4 was isolated and free PMe_2Ph added to increase the percentage of 3. The composition of this solution was established by ^{31}P NMR spectroscopy and it was then irradiated (THF solution). The resulting yellow solid, isolated in low yield, was identified as the phosphide 7. It was established that the conversion of 3 to 7 does not involve 6 as an intermediate since isolated 6 showed no reaction when irradiated for 16 h in CH_3CN. Such cleavage of a P–CH_3 bond has never before been observed at 25 °C.[28]

The proposed conversion of 3 to 6 is more difficult to prove. We have seen that protonation of 3 leads to the cation of 6 ($Os_2H_3P_6^+$) in high yield, so the notion that 3 is a precursor to 6 is not unreasonable. However, the anion in 6 ($OsH_4P_2^-$) would seem to arise from reaction of 3 with some monomeric osmium species. On the basis of the number of phosphine ligands, $OsH_4P_2^-$ could be derived from either (A) the photoproduct OsH_6P_2 or (B) the phototransient OsH_4P_2, either of which might be reduced to $OsH_4P_2^-$ via an electron-transfer process. For OsH_6P_2 (case A), the indicated test experiment involves photolysis of $Os_2H_4P_6$ (3) together with OsH_6P_2 (and in the absence of any OsH_4P_3). However, the presence of 3 generates equilibrium concentrations of free PMe_2Ph. Consequently, the result of this irradiation experiment was simply conversion of OsH_6P_2 to OsH_4P_3 (eq 14). While this reaction

$$OsH_6P_2 + P \xrightarrow{h\nu} OsH_4P_3 + H_2 \qquad (14)$$

indicates the photochemical behavior of OsH_6P_2 (i.e. H_2 loss), it obscures the answer to the original question. However, indirect evidence bears on the possible conversion of 3 to 6. If the photochemistry of OsH_4P_3 is monitored over time via ^{31}P NMR spectroscopy, one observes the initial production of 3. Eventually, the percentage of 3 reaches a maximum and begins to decrease, an event that is followed closely by the appearance of 6. This is a necessary (but not sufficient) condition related to the hypothesis that 6 is produced from 3. Another observation bears on this issue and on the surprising formation of ionic 6 in dilute benzene. High concentrations of OsH_4P_3 lead to a reduced fraction of the products being 6, even in benzene. We believe that the production of 6 is more dependent on concentration than on solvent (recall that 7 was initially observed and isolated from a photolysis in dilute benzene). In concentrated solutions, the majority of the 3 produced is immediately precipitated and is thus unavailable for further reaction. However, in dilute solution the available 3 remains dissolved and can undergo subsequent photochemistry. Thus, 6 and 7 are a large percentage of the total product spectrum upon longer photolysis in dilute solution since the number of photons passed through the solution *per osmium dissolved* is greater under these conditions. The partitioning of 3 between formation of 6 vs 7 is then dictated by the presence or absence of the monomeric species that is the precursor of $OsH_4P_2^-$ in 6.

(26) Venanzi, L. M. *Coord. Chem. Rev.* **1982**, *43*, 251.
(27) Muralidharan, S.; Ferraudi, G.; Green, M.; Caulton, K. G. *J. Organomet. Chem.* **1983**, *243*, 47.
(28) Garrou, P. *Chem. Rev.* **1985**, *85*, 171.

Nature of the Excited States. The participation of two photochemical pathways following excitation of OsH_4P_3 raises questions regarding the nature of the excited state or states responsible. In their study of the photochemistry of MH_4P_4 (M = Mo, W) Wrighton and Geoffroy considered[29] excited states that are metal-to-phosphine charge transfer (MLCT) as well as those that are M–H_2 σ^* in nature. Similarly, the active state in IrH_3P_3 was also identified as M–H_2 σ^* in nature.[30] In both of these systems, the result was photoextrusion of H_2. In OsH_4P_3, the UV–visible spectrum contains a band at 282 nm whose intensity (ϵ = 5400 L/(mol cm)) suggests a charge-transfer transition. We have employed the qualitative molecular orbital picture described below to understand this.

The MO picture for a regular ML_7 pentagonal bipyramid (with seven σ-bonding ligands) has been described.[31] It consists of a low-lying $e_{1''}$ (xz, yz) set, which is nonbonding, and two metal–ligand antibonding sets of $e_{2'}$ (xy, $x^2 - y^2$) and $a_{1'}$ (z^2) symmetry. In a d^4 system such as OsH_4P_3, the low-lying $e_{1''}$ set is filled. The actual symmetry of OsH_4P_3 is C_{2v}, with the C_2 axis containing Os and the equatorial phosphine. If we ignore π-bonding effects, symmetry lowering allows us to assign the orbitals in C_{2v} terms by analogy with the regular ML_7 pentagonal bipyramid (D_{5h}). This procedure results in two low-lying filled orbitals of a_2 and b_1 symmetry (nonbonding), a set of two antibonding orbitals of a_1 and b_2 symmetry, and a high-lying antibonding orbital of a_1 symmetry. Both of the a_1 orbitals are metal–phosphine σ^* orbitals, and the b_2 orbital is a metal hydride σ^* antibonding orbital. If the observed UV band involves two unresolved excitations, each being allowed and being from a largely nonbonding metal d orbital to the M–H_2 σ^* (a_1) orbital and to a M–P σ^* (b_2) orbital, the two observed photodissociations can be rationalized.

Aggregation Process. The mechanism by which monomeric osmium species condense to dimers appears to involve reaction of the 16-electron transient OsH_2P_3 with the starting material. This mechanism involves reaction of a saturated polyhydride with an unsaturated moiety and has ample precedent. Venanzi has shown that species of general formula $P_2Pt(R)(S)^+$ (S = weakly bound solvent) undergo loss of S, followed by facile binding to saturated hydride species such as Cp_2WH_2[32] or PtH_2P_2.[32] Likewise, $PAu(THF)^+$ loses THF and condenses with *mer*-IrH_3P_3.[33] All of these dimers contain one or more μ-H linkages. Similarly, we[34] and Bulychev[35] have shown that the compounds Cp_2MH_2 (M = Mo, W) will react with numerous Lewis acids to form adducts, many of which are held together by bridging hydrides. We have also seen that saturated ReH_7P_2, ReH_5P_3, and IrH_3P_3 will react with sources of "naked" Cu(I) to form a variety of metal–copper adducts involving primary bonding of copper to bridging hydrides.[36] All of these reactions are facilitated by the ease with which terminal hydride ligands can adopt a three-center, two-electron bridging mode. Indeed, this is graphically illustrated by the equilibrium interconversion of **3** and **4**, in which a terminal hydride in **3** becomes a bridging hydride in **4** (eq 9).

We have noted that the conversion of two OsH_4P_3 species into $Os_2H_4P_6$ (**3**) requires the loss of **2** equiv of H_2. Yet if the reaction does proceed via combination of OsH_4P_3 and OsH_2P_3, the initially formed dimer should have six hydride ligands, "$Os_2H_6P_6$". Such a compound is never observed, even though it could satisfy the effective atomic number rule with a single Os–Os bond (as does **1**). Compounds **3** and **4** also fail to undergo any reaction with H_2 under forcing conditions (1000 psi of H_2); there is no addition of H_2 across the metal–metal bonds, a reaction that has been observed in some tantalum dimers.[37] The feature common to all of the dimeric osmium compounds reported here is the achievement of octahedral coordination geometry. Normally, this geometry is achieved within the constraints of the EAN rule, which is satisfied by metal–metal bonding. While it is not surprising that a d^6 Os(II) center prefers octahedral geometry, we have also seen this preference in the phosphide-bridged **7**, which is formally a d^5–d^5 dimer. Even more spectacular is the facile formation of *trans*-$OsH_4P_2^-$ in **6**. This Os(III) anion is a d^5, 17-electron species, indicating that, at least in this case, the tendency toward an octahedron is more important than the EAN rule (which has never before been violated in polyhydrides of osmium). This factor must be considered the driving force for production of this novel paramagnetic polyhydride.

Conclusions. This work reveals the first example of a polyhydride that undergoes two distinct photoprocesses (H_2 and phosphine extrusion) with comparable efficiencies. This appears to be a consequence of the accidental near-degeneracy of two chemically quite distinct excited states. The resulting 16-electron transients are capable of effecting H/D exchange with solvent, and they can be trapped with scavengers such as H_2 and PR_3. In the absence of scavengers, OsH_4P_3 is seen to result in a dimeric product that is reactive in both thermal and photochemical reactions; a mechanistic sequence is proposed to account for these transformations. The production of a novel paramagnetic polyhydride radical anion also prompted a synthetic inquiry leading to the facile production of other (diamagnetic) polyhydride anions. Photochemistry has proven to be a route to several hydride-rich dimers with varying osmium–osmium bond orders.

Experimental Section

General Considerations. All solvents were dried with use of Na/K alloy and then vacuum-transferred. Photolyses were conducted with a Hanovia 550-W medium-pressure Hg lamp or a Photochemical Research Associates 100-W high-pressure Hg lamp in quartz glassware. ^{31}P NMR spectra were recorded at 40.5 MHz on a Varian XL-100 spectrometer, while ^1H NMR spectra were recorded at 360 MHz on a Nicolet spectrometer or at 220 MHz on a Varian spectrometer. All NMR data are given in units of δ, with J values being in Hz. For crystallographic procedures, see ref 38.

$OsCl_3(PMe_2Ph)_3$. Two $^1/_2$-g ampules of OsO_4 were broken open and dropped into 30 mL of absolute ethanol and 1.8 mL of concentrated HCl in an Erlenmeyer flask, and the solution was stirred to dissolve the OsO_4. The solution was then poured into a 200-mL round-bottom flask and an additional 15 mL of EtOH added. The yellow solution was degassed by three freeze–pump–thaw cycles and 3 mL of PMe_2Ph added against a rapid flow of N_2, causing the solution to turn dark red. The mixture

(29) Graff, J. L.; Sobieralski, T. J.; Wrighton, M. S.; Geoffroy, G. L. *J. Am. Chem. Soc.* **1982**, *104*, 7526.
(30) Geoffroy, G. L.; Pierantozzi, R. *J. Am. Chem. Soc.* **1976**, *98*, 8054.
(31) Hoffmann, R.; Beier, B. F.; Muetterties, E. L.; Rossi, A. R. *Inorg. Chem.* **1977**, *16*, 511.
(32) Albinati, A.; Naegeli, R.; Togni, A.; Venanzi, L. M. *Organometallics* **1983**, *2*, 926.
(33) Albinati, A.; Desmartin, F.; Janser, P.; Rhodes, L. F.; Venanzi, L. M. *J. Am. Chem. Soc.* **1989**, *111*, 2115.
(34) Bruno, J. W.; Huffman, J. C.; Caulton, K. G. *J. Am. Chem. Soc.* **1984**, *106*, 444.
(35) Soloveichik, G. L.; Bulychev, B. M. *Russ. Chem. Rev.* (*Engl. Transl.*) **1983**, *52*, 72.
(36) Rhodes, L. F.; Huffman, J. C.; Caulton, K. G. *J. Am. Chem. Soc.* **1985**, *107*, 1759.
(37) Sattelberger, A. P.; Wilson, R. B.; Huffman, J. C. *Inorg. Chem.* **1982**, *21*, 4179.
(38) Huffman, J. C.; Lewis, L. N.; Caulton, K. G. *Inorg. Chem.* **1980**, *19*, 2755.

was refluxed for 2 h and the red crystalline $OsCl_3(PMe_2Ph)_3$ isolated by filtration after cooling to room temperature. Product identity was established by a comparison to the literature ^1H NMR spectrum; yield 1.74 g, 75%. Additional product crystallized from the ethanol filtrate upon allowing it to stand in the open filter flask for a few days.

$OsH_4(PMe_2Ph)_3$. To 1.74 g of $OsCl_3(PMe_2Ph)_3$ in 75 mL of ethanol was added 1.5 g of $NaBH_4$ against a flow of N_2. The mixture, which became colorless after stirring for ~10 min at room temperature, was refluxed for 1 h and then evaporated to dryness. The colorless residue was extracted with 4 × 40 mL of C_6H_6 and the yellow benzene solution evaporated to leave a yellow oil. This yellow oil gave $OsH_4(PMe_2Ph)_3$ as a white powder (1 g) upon washing with ~15 mL of absolute ethanol. Evaporation of the ethanol mother liquor gave a sticky white solid, which ^1H and ^{31}P NMR spectra showed also to be $OsH_4(PMe_2Ph)_3$ with no detectable impurities. ^1H NMR (360 MHz, C_6D_6): 7.53 (m, ortho C_6H_5), 7.03 (m, meta and para C_6H_5), 1.63 (1:1:1 "t", J = 4, P–CH_3), −8.98, (J = 10, Os–H). $^{31}P\{^1H\}$ NMR (30 °C): −28.6 (with ^{187}Os ($I = {}^1/_2$) satellites, $^1J(^{187}Os–^{31}P)$ = 165).

***cis*-$OsH_2(PMe_2Ph)_4$.** A saturated benzene solution of $OsH_4(PMe_2Ph)_3$ and 3 equiv of PMe_2Ph were photolyzed in an NMR tube for 1 h. ^{31}P NMR spectroscopy shows 50% conversion to *cis*-$OsH_2(PMe_2Ph)_4$, with no other products. As reported,[7] heating a similar toluene solution of $OsH_4(PMe_2Ph)_3$ and PMe_2Ph to 100 °C for 20 h also gives clean conversion to *cis*-$OsH_2(PMe_2Ph)_4$. ^1H NMR (220 MHz, C_6D_6): 7.84 (t, J = 7, *o* phenyl), 7.66 (br t, J = 7, *o* phenyl), 7.14 (m, *m* + *p* phenyl), 1.68 (t, J = 3, CH_3), 1.50 (d, J = 6, CH_3), −10.48 (multiplet, OsH). $^{31}P\{^1H\}$ NMR: −31.7 and −33.8, each a triplet with J = 15.

$Os_2H_4(PMe_2Ph)_6$ (3). This product precipitated as dark red crystals from the supersaturated solutions that result from the photolysis of saturated benzene or THF solutions of $OsH_4(PMe_2Ph)_3$. ^1H NMR (360 MHz in toluene-d_8, obtained after addition of a large excess of PMe_2Ph to $Os_2H_4(PMe_2Ph)_6$, to shift the equilibrium): 1.70 (br s, 1), 1.48 (br s, 2); a broad hydride resonance at −13.6 ppm could not be accurately integrated because of low S/N. $^{31}P\{^1H\}$ NMR (THF): 0.6 (br s, 1 P, $\Delta\nu_{1/2}$ = 15 Hz), −26.7 (br s, 2 P, $\Delta\nu_{1/2}$ = 10 Hz).

Single-Crystal X-ray Diffraction Study of $Os_2H_4(PMe_2Ph)_6$. A suitable crystal was transferred to the goniostat with use of standard inert-atmosphere handling techniques. A systematic search of a limited hemisphere of reciprocal space located diffraction maxima that could be indexed as monoclinic, space group $P2_1/a$, and subsequent solution and refinement confirmed this choice. Parameters of the unit cell and data collection ($5° \le 2\theta \le 50°$) are shown in Table I. The data were corrected for absorption. The structure was solved by direct methods (MULTAN78) and Fourier techniques and refined by full-matrix least-squares methods. A difference Fourier synthesis phased on the non-hydrogen atoms clearly located all hydrogen atoms, although there were several peaks located in the vicinity of the osmium atom. Refinement continued with the inclusion of all but the bridging hydrogen atoms, with use of isotropic thermal parameters for the hydrogens and anisotropic thermal parameters for non-hydrogen atoms. At this stage a difference Fourier map gave three peaks of height ca. 1.8 e/Å^3, one located 0.2 Å from the Os and the other two 0.9 Å from the Os in the direction of two of the phosphorus atoms. The fifth largest peak (0.85 e/Å^3) was located in a bridging position and was refined accordingly. While the refined distances to the bridging hydrogen are clearly asymmetric, this is not surprising, considering the proximity of the Os atoms. A final difference map still exhibited the three peaks mentioned above, presumably artifacts of inaccurate scattering terms for the Os or absorption correction errors. The results of the structure determination are shown in Table II and Figure 2. Additional information is available as supplementary material.

$Os_2H_4(PMe_2Ph)_5$ (4). Photolysis of a saturated ethanol solution of $OsH_4(PMe_2Ph)_3$ for 4 h led to deposition of orange crystals that a ^{31}P NMR spectrum in C_6H_6 reveals to be a mixture of $Os_2H_4(PMe_2Ph)_n$ (n = 5, 6). The relative amount of $Os_2H_4(PMe_2Ph)_5$ was dramatically increased by heating the sample in benzene to 80 °C in a round-bottom flask and then removing the solvent and liberated PMe_2Ph as quickly as possible in vacuo. $^{31}P\{^1H\}$ NMR (toluene-d_8): −14.7 (q, J = 5), −19.0 (t, J = 5). Both resonances are further split into complex multiplets upon selective coupling to hydride hydrogens. ^1H NMR (360 MHz): 8.05 (t, J = 8, *o* phenyl), 7.80 (t, J = 8, *o* phenyl), 7.1 (complex m, *m* + *p* phenyl), 1.88 (two unresolved d), 1.47 (d, J = 7), −8.95 (v br apparent doublet, Os–H).[15]

Photolysis of $OsH_4(PMe_2Ph)_3$ under H_2 Pressure. The photoreactor was charged with 1 mL of THF, 0.07 g (0.12 mmol) of $OsH_4(PMe_2Ph)_3$, and 60 atm of H_2. The solution was photolyzed through a quartz window for 26 h. The reactor was carefully vented, and the $^{31}P\{^1H\}$ NMR spectrum of the resulting solution revealed only two singlets, that of $OsH_6(PMe_2Ph)_2$ at −29.9 ppm and that of PMe_2Ph at −48 ppm. The orange solution was taken to dryness under vacuum at 25 °C, and PMe_2Ph was washed away from the residue with use of cold hexane. ^1H NMR (C_6D_6): 7.57 (m, *o* phenyl), 7.2–6.9 (m, *m* + *p* phenyl), 1.59 (d, J = 10, 12 H), −8.59 (t, J = 5, 6 H).

Photolysis of Dimers under H_2. A 0.08-g sample of $OsH_4(PMe_2Ph)_3$ was photolyzed in 1 mL of THF until consumption of reagent was 95% complete (by ^{31}P NMR). The resulting solution, containing PMe_2Ph, $Os_2H_4P_5$, and $Os_2H_4P_6$, was transferred to the photoreactor and irradiated for 24 h under 60 atm of H_2. The photoreactor was carefully vented, revealing a yellow solution and a yellow solid. The ^{31}P NMR spectrum of the solution showed a weak signal (compared to that of free PMe_2Ph) of OsH_6P_2 and a still weaker signal at −21.9 ppm due to the cation in the poorly soluble compound $[Os_2H_3P_6][OsH_4P_2]$. The yellow solid also formed in this reaction is $[Os_2H_3P_6][OsH_4P_2]$ as well (identified by IR spectroscopy).

$K[OsH_5(PMe_2Ph)_2]$. Approximately 150 mg (0.32 mmol) of $OsH_6(PMe_2Ph)_2$ (as an oil) was taken up in 10 mL of THF. This solution was dripped into a 10-mL slurry of excess KH (25 mg, 0.62 mmol) in THF. Gas evolution was moderate and ceased after 10 min at 25 °C, at which time the solution was filtered to remove unreacted KH. The solvent was then removed in vacuo and the residue dissolved in a minimum volume of CH_3CN. Cooling resulted in orange microcrystals. ^1H NMR (CD_3CN): 7.15, 7.26 (m, P–Ph), 1.77 (d, J = 6 Hz, P–Me), −11.2 (t, J = 11 Hz, Os–H). $^{31}P\{^1H\}$ (CD_3CN): −27.4 (s). Selective coupling to upfield Os–H gives a ^{31}P NMR sextet with J = 11 Hz. IR (Nujol): 1955 m, 1942 m, 1728 m cm^{-1}.

$K[fac$-$OsH_3(PMe_2Ph)_3]$. To a THF solution of 50 mg of $OsH_4(PMe_2Ph)_3$ in an NMR tube was added excess KH powder (prepared from a 35% mineral oil dispersion of KH, as described earlier).[17] The NMR tube was sealed with a flame, and the reaction mixture was heated at 70 °C in an oil bath for 12 h. ^{13}P and ^1H (from reaction in THF-d_8) NMR spectra showed quantitative conversion to yellow $K[fac$-$OsH_3(PMe_2Ph)_3]$. $^{31}P\{^1H\}$ NMR (THF-d_8): −30.1 (s). ^1H NMR (220 MHz, 16 °C, THF-d_8): 7.89 (t, J = 7, 6 H), 7.20 (m, 9 H), 1.54 (d, J = 6, 18 H), −11.60 (AA′A″XX′X″ multiplet, 3 H). This compound has also been characterized by X-ray diffraction.[17] While KH is easily removed by filtration, flame-dried glassware is essential to preventing the anion from reprotonating to give OsH_4P_3. Addition of H_2O to a THF solution of the anion gave immediate (^{31}P NMR) conversion to OsH_4P_3.

$OsH_4(PEt_3)_3$. To a slurry of 1.5 g (2.31 mmol) of $OsCl_3(PEt_3)_3$ in 40 mL of EtOH was added 1.0 g of $NaBH_4$. The solution was refluxed 1 h, leading to a color change from red to colorless. The reaction mixture was stripped of solvent under vacuum and extracted with 5 × 30 mL of benzene to give a pale yellow solution. Concentration of this filtered solution to 5 mL, and addition of MeOH, gave a colorless solid, yield 0.71 g (61%). ^1H NMR (C_6D_6): 1.45 (br m, CH_2), 0.98 (br m, CH_3), −11.0 (q, J = 10, OsH). $^{31}P\{^1H\}$ NMR (THF): 0.3 (s).

$OsH_6(PEt_3)_2$. A sample of 0.05 g of $OsH_4(PEt_3)_3$ in 3 mL of benzene was photolyzed for 25 h under 60 atm of H_2. The product was isolated as a phosphine-free yellow oil. ^1H NMR (C_6D_6): 2.0–1.0 (complex m, PEt_3), −9.7 (t, J = 5, Os–H). $^{31}P\{^1H\}$ NMR (THF): 11.5 (s).

$OsH_4(PMePh_2)_3$. This compound was prepared from 1.3 g of $OsCl_3(PMePh_2)_3$, as were the tetrahydrides of PEt_3 and PMe_2Ph. The yield was 0.8 g (61%). ^1H NMR (C_6D_6): 7.61 (m, o phenyl), 6.98 (m, *m* + *p* phenyl), 1.88 (br s, Me), −8.41 (q, J = 10, OsH). $^{31}P\{^1H\}$ NMR (THF): −5.3 (s).

$Os_2H_4(PMePh_2)_5$ (5). A THF solution containing 0.10 g of $OsH_4(PMePh_2)_3$ was irradiated in a quartz tube for 20 h. The

course of the reaction was monitored by ^{31}P NMR spectroscopy; the solution color changes from pale yellow to red-orange during photolysis. After 20 h, the only phosphorus NMR signals were those of $Os_2H_4(PMePh_2)_5$ and free $PMePh_2$. The solution was evaporated to dryness, dissolved in toluene, and concentrated to 0.1 mL, and 0.5 mL of acetonitrile was added. When the solution stood at −20 °C for 2 days red-orange crystals formed (used in the X-ray study). ^1H NMR (360 MHz, C_6D_6): 7.98 (br m, 4 H), 7.75 (br m, 4 H), 7.53 (br m, 12 H), 7.1–6.8 (complex m, 30 H), 1.82 (virtual t, J = 6, 6 H), 1.61 (d, J = 8, 9 H), −8.9 (br d, J = 46, 3 H), −20.1 (t, J = 26, 1 H). $^{31}P\{^1H\}$ NMR (THF): 6.2 (q, J = 6, 2 P), −1.9 (t, J = 6, 3 P).

X-ray Diffraction Study of $Os_2H_4(PMePh_2)_5$. A suitable sample was transferred to the goniostat with use of standard inert-atmosphere handling techniques and cooled to −162 °C. A systematic search of a limited hemisphere of reciprocal space revealed a monoclinic lattice that could be indexed as $P2_1/c$. Parameters of the unit cell and data collection ($6° \le 2\theta \le 45°$) are given in Table I. The structure was solved by direct methods (MULTAN78) and Fourier techniques. After blocked full-matrix refinement of the non-hydrogen atoms, a difference Fourier map clearly located all non-hydridic hydrogens. The latter were then added to the model and refinement was continued, with isotropic thermal parameters for hydrogen atoms and anisotropic thermal parameters for non-hydrogen atoms. A difference Fourier map phased on this final model contained four peaks of intensity 1.1–1.7 e/Å^3, all located within 0.7 Å of the two Os atoms. In addition, several peaks of intensity 0.6–0.8 e/Å^3 were located in positions that are chemically reasonable for hydridic hydrogens. No attempt was made to refine the latter due to the close proximity of two of the bridging hydrogens to two of the larger residuals in the final difference Fourier map. ψ scans of six reflections indicated the maximum error due to absorption was 5%, so no attempt was made to correct the data. The results of the structure determination are shown in Table III and Figure 3. Table III shows distances and angles for the (unrefined) peaks H(A)–H(D) in the final difference map which might be assigned as hydrogens. Additional information is available as supplementary material.

Photolysis of $OsH_4(PEt_3)_3$. A C_6D_6 solution (1 mL) of 0.05 g (0.09 mmol) of $OsH_4(PEt_3)_3$ was irradiated in a quartz NMR tube for 2 h. Although the proton NMR chemical shifts remained unchanged, integration of the ^1H NMR signals against an internal intensity standard showed the growth of C_6D_5H and a 50% reduction in Os–H. The ethyl CH_2 multiplet remained unchanged. The phosphorus chemical shift moved 0.1 ppm downfield in the deuterated complex and was broadened by P–D coupling.

To evaluate the effect of added PEt_3 on this exchange, $OsH_4(PEt_3)_3$ (0.1 g, 0.18 mmol), PEt_3 (0.1 mL, 0.68 mmol), and 0.5 mL of C_6D_6 were sealed into a quartz NMR tube. With internal TMS as an intensity standard, 30% loss of Os–H ^1H NMR intensity was observed after 5 h of irradiation. After addition of an additional 0.3 mL (2.04 mmol) of PEt_3 to this solution, irradiation for 5 h showed no further deuteration of Os–H bonds. Note also that this solution (free PEt_3/Os = 15) showed no production of $OsH_2(PEt_3)_4$.

$[Os_2H_3(PMe_2Ph)_6]Cl$. A saturated benzene solution of $OsH_4(PMe_2Ph)_3$ was diluted with a 7-fold excess of benzene and photolyzed for 3 h in a 7 mm i.d. quartz tube. The yellow crystalline product was isolated by filtration and recrystallized from CH_2Cl_2/Et_2O, giving the chloride salt (established by X-ray diffraction). $[Os_2H_3(PMe_2Ph)_6][BF_4]$ was prepared by adding excess $HBF_4 \cdot Et_2O$ to a THF suspension of $Os_2H_4(PMe_2Ph)_6$. NMR data for $[Os_2H_3(PMe_2Ph)_6]Cl$ in CD_2Cl_2: $^{31}P\{^1H\}$ NMR (30 °C) −21.9 (s) (doublet, with an apparent J_{PH} of 16 Hz, upon selective decoupling of only the downfield protons); ^1H NMR (360 MHz, 23 °C) 8.18 (br, s, *o* C_6H_5), 7.55 (*m* and *p* C_6H_5), 1.62 (br s, P–CH_3), −9.45 (vbr s, Os–H). ^{31}P and ^1H NMR spectra of the yellow crystals isolated for photolysis in benzene (i.e. $[Os_2H_3P_6][OsH_4P_2]$) were recorded in methylene-d_2 chloride, acetone-d_6, and acetonitrile-d_3 and in no case exhibited resonances that could be assigned to the anion which must be present; only the resonances of the cation were evident.

X-ray Diffraction Study of $[Os_2H_3(PMe_2Ph)_6][OsH_x(PMe_2Ph)_2]$. A suitable crystal was cleaved from a large clump and transferred to the goniostat with use of standard inert-atmosphere handling techniques. A systematic search of a limited hemisphere of reciprocal space revealed a monoclinic lattice with extinctions corresponding to space group $C2/c$. Subsequent solution and refinement of the structure confirmed this choice. Parameters of the unit cell and data collection ($5° \le 2\theta \le 50°$) are shown in Table I. The data were corrected for absorption. The structure was solved by direct methods (MULTAN78) and Fourier techniques and refined by full-matrix least squares. All hydrogen atoms with the exception of the anion hydridic hydrogens were located and refined. A final difference Fourier map was featureless, the largest peak being 0.75 e/Å^3. The results of the structure determination are shown in Table IV and Figure 4. Additional information is available as supplementary material.

$Os_2H_4(PMe_2Ph)_4(PMePh)_2$. The orange benzene mother liquor from the above reaction, which yielded crystals of $[Os_2H_3(PMe_2Ph)_6][OsH_4P_2]$, was evaporated to dryness and the orange residue redissolved in a minimum of benzene. This solution was filtered and concentrated further. The phosphide complex deposited as orange crystals when this benzene solution stood at room temperature. ^1H NMR (220 MHz in CD_2Cl_2, in addition to many phenyl resonances): 2.11, (d, J = 8, P–CH_3), 1.99, (d, J = 8, P–CH_3), 1.91 (d, J = 8, P–CH_3), 0.77 (d, J = 5, P–CH_3), 0.63 (d, J = 5, P–CH_3), −9.5 (br t, J = 40, Os–H), −15.3 (vbr d, $J \approx 80$, Os–H). The five methyl resonances are of equal intensity. $^{31}P\{^1H\}$ NMR (THF): 126.9 (d (116.6 Hz) of multiplets, PMePh), −34.3 ("pseudodoublet", J = 116.6, $PMe_2$3Ph), −44.6 (t, J = 12, PMe_2Ph). All have equal intensity.

X-ray Diffraction Study of $Os_2H_4(PMe_2Ph)_4(PMePh)_2$. With use of standard inert-atmosphere handling techniques, a small fragment of a diamond-shaped plate was transferred to the goniostat, where it was cooled to −165 °C. The sample was very irregular in shape, and no absorption correction was performed. The crystals are thermochromic, turning from a deep orange at 18 °C to bright yellow at −165 °C. The space group was assigned with use of a standard reciprocal lattice search technique. Parameters of the unit cell and data collection ($6° \le 2\theta \le 50°$) are shown in Table I. The structure was solved by a combination of direct methods (MULTAN78), Patterson functions, and Fourier techniques. All atoms were refined by full-matrix least squares, and hydrogen atoms, including the hydrides, were located in a difference Fourier synthesis phased on the non-hydrogen parameters. Final refinement included all hydrogen atoms with isotropic thermal parameters. A final difference Fourier synthesis produced one peak of height 2.3 e/Å^3 at the Os position and two other peaks of intensity 1.4 and 1.3 e/Å^3 between Os and P(2) and P(3). All other peaks were less than 0.8 e/Å^3 and were evenly distributed throughtout the cell. The results of the structure determination are shown in Table V and Figure 5. Additional crystallographic details are available as supplementary material.

Acknowledgment. This work was supported by the National Science Foundation. We thank Johnson Matthey, Inc., for material support and Scott Horn for skilled technical assistance.

Supplementary Material Available: Listings of crystal data, anisotropic thermal parameters, and positional parameters for $Os_3H_4(PMe_2Ph)_6$, $Os_2H_4(PMePh_2)_5$, $[Os_2H_3(PMe_2Ph)_6][OsH_4(PMe_2Ph)_2]$, and $Os_2H_4(PMe_2Ph)_4(PMePh)_2$ (16 pages); listings of observed and calculated structure factors (106 pages). Ordering information is given on any current masthead page.